

## **Probing the Influence of the Power Deposition Profile on Impurity Transport by Injecting Silicon into the TJ-II Stellarator**

B. Zurro, M. A. Ochando, A. Baciero, R. Dux\*, A. Fernández, A. Cappa, V. Tribaldos, K. J. McCarthy, F. Medina, A. López-Sánchez, D. Jiménez, D. Rapisarda, I. Pastor, J. Herranz, and TJ-II Team.

*Laboratorio Nacional de Fusión, Asociación Euratom-CIEMAT, Madrid, Spain.*

*\*Max Planck Institut für Plasmaphysik, Garching (Germany).*

**Introduction.** Impurity confinement studies have been performed in several stellarator devices by either injecting them by laser ablation or by pellets. When the perturbation relaxation is considered only, one can deduce the impurity confinement time from its decay constant. Such studies have been performed in several stellarators, in particular in the W-7 AS [1] where these have been carried out in some detail [1] and [2] and, where an impurity confinement scaling law for was determined as function of density, injected power, etc.. However, and as far as we know, the dependence of impurity transport when changing from on-axis to off-axis electron cyclotron resonance heating (ECRH) has not been studied in stellarator devices. In contrast, such studies have been performed in tokamaks for a full battery of heating schemes [3]. The analysis with spatial resolution of impurity injection experiments in stellarators has been carried out using the evolution of soft x-ray signals [2], visible bremsstrahlung signatures [4] or bolometric reconstructed perturbations [5], the latter is used here.

In this paper, impurity injection experiments performed by the laser ablation technique have been made in ECRH plasmas of the TJ-II stellarator in order to probe the influence of the heating deposition profile on impurity transport. This experiment was motivated by the transport results obtained in a previous ECRH power scan experiment which showed a diffusion coefficient decreasing with radii and increasing with injected power [6]. This paper is organized as follows. First, we describe briefly the experimental set-up and TJ-II discharges employed for this experiment. Second, we present the results of an analysis of chord integrated radiation monitors and tomographically reconstructed signals fitted by stretched exponentials, i.e. by the expression  $A_1 \exp[-((t-t_0)/\tau)^\beta]$ .

**Experimental.** The TJ-II is a four-period, low magnetic shear, stellarator with a major and averaged minor radii of 1.5 m and  $a \leq 0.22$  m, respectively. At present, central electron densities and temperatures up to  $1.7 \times 10^{19} \text{ m}^{-3}$  and 2 keV respectively are achieved for

plasmas created and maintained by ECRH at second harmonics ( $f = 53.2$  GHz,  $P_{\text{ECRH}} \leq 600$  kW).

The laser ablation system is described in more detail in ref. [5]. Here, silicon tracer ions were injected into almost stationary phases of ECRH plasmas using the laser ablation technique. For this, a thin film of material ( $2 \mu\text{m}$  Si), deposited onto the surface of a glass substrate, was ablated by the short pulse of a focused Q-switched Nd-YAG laser beam (800 mJ, 10 ns).

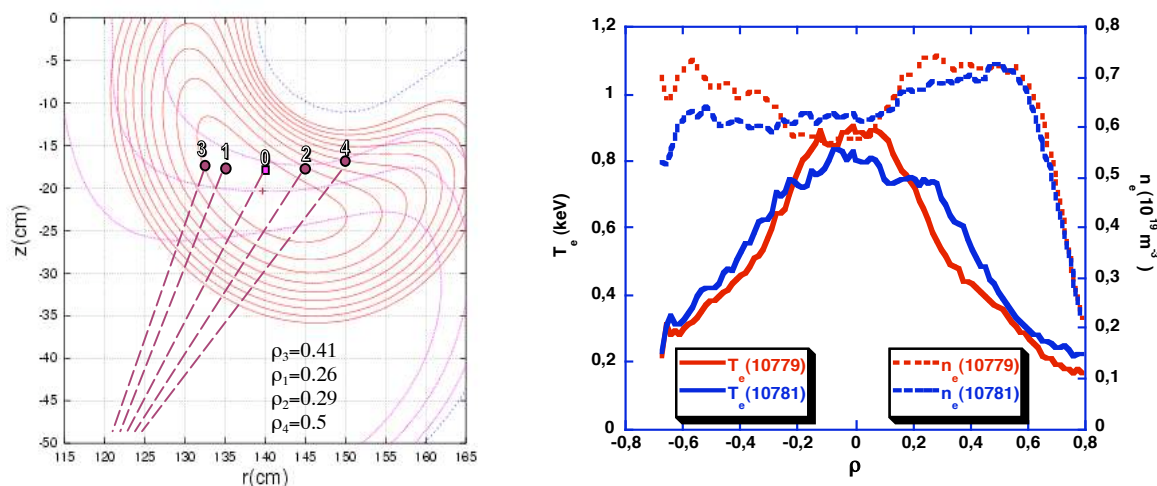


**Fig. 1.** *Left*, the contours of constant  $|B|$  and magnetic surfaces of the TJ-II standard configuration (100\_44\_64) showing the positions where the power deposition scan was performed. *Right*, comparison of Thomson scattering profiles for two discharges with on-axis heating (10779) and off-axis heating (10781).

The present experiment was performed by creating almost constant electron density discharges in hydrogen for a standard TJ-II magnetic configuration, and modifying, on a shot-to-shot basis, the position and width of the ECRH power deposition profile. The location of the power deposition is controlled by adjustment of the toroidal field or by poloidal and/or toroidal steering of the launched beam at fixed magnetic field. The latter has been the method employed here. For this, approximately 400 kW of power were launched at different plasma radii from the centre out to around  $\rho \approx 0.5$ , the beam waist in vacuum is 1 cm. See Fig. 1 where the different positions and geometrical paths in vacuum of the electron cyclotron beam during this experiment are shown.

In Fig. 1 right, we compare electron temperature (lines) and density (dashed lines) profiles for two discharges, one with on-axis ECR heating (red) the other with off-axis heating (blue). Standard discharge monitors are depicted in Fig. 2 for these discharges.

**Results and discussion.** A first analysis of impurity confinement, determined from the relaxation of the signatures of central chord-integrated global radiation detectors fitted by a stretched exponential is shown in Fig. 3. On the vertical axis of the left-hand-side, we plot the decay times of a central chord x-ray detector (open circles) and a central chord

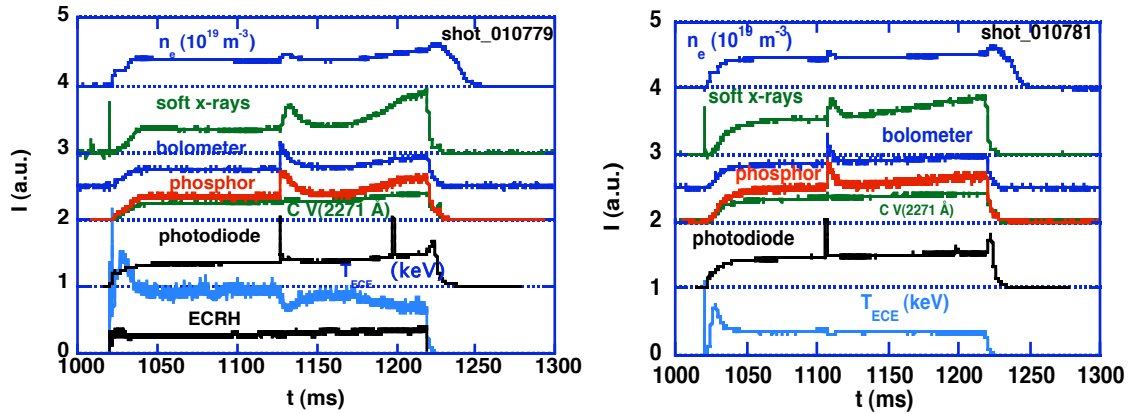


**Fig. 2.** Comparison of two discharges: on the left one with on-axis heating and on the right one with off-axis heating. From top to bottom the signatures represent line-averaged electron density, soft x-ray monitor, various radiation monitors and ECE electron temperature.

phosphor detector (filled points) sensitised to the whole VUV range, while on the horizontal axis we plot the ECRH launching mirror angle which is the main knob used to modify the ECRH power deposition.

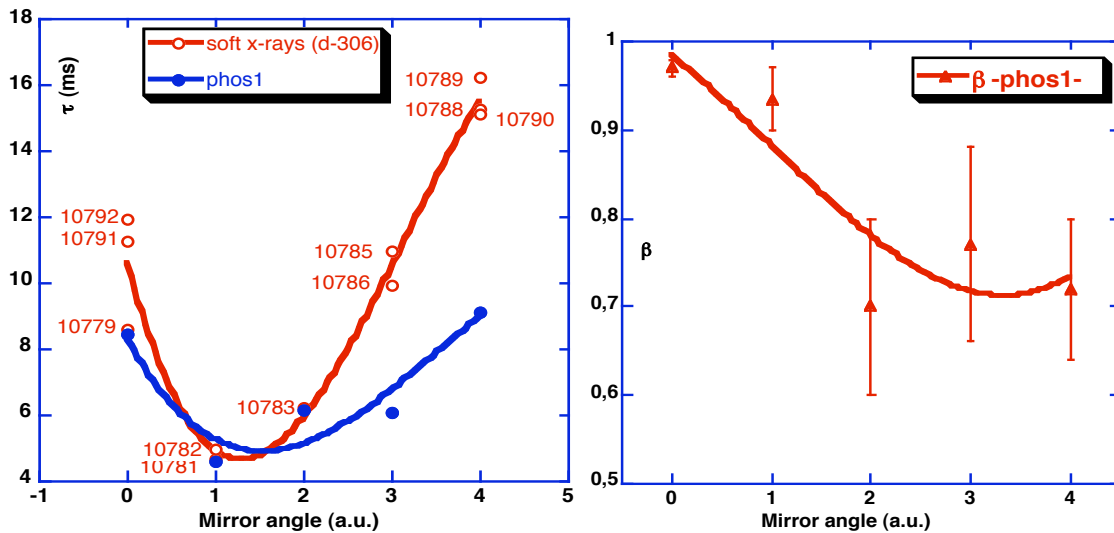


**Fig. 3.** *Left.* Impurity confinement time behaviour deduced from the soft x-ray central channel ( $E_{ph} > 1-2$  keV) and a central chord channel of a global VUV monitor. *Right,*  $\beta$  parameter of the stretched exponential deduced from the phosphor detector signature.

In Fig. 3 right, we display a similar plot for the beta parameter deduced from the relaxation in the VUV luminescent detector. In addition to the previous analysis carried out with

chord-integrated signals, which highlights in a simple way the clear effect produced by this scan, a more detailed analysis was performed with the local reconstructed time evolution of the impurity injection provided by bolometer and soft x-ray detector arrays. In Fig. 4, we show the results of this analysis for three discharges where the nominal centre of the ECR heating was tuned to effective radii 0, 0.26 and 0.5, respectively. We see similar results to those manifested by the simpler analysis, the decay time shows a minimum for intermediate position and the beta parameter goes from values close to one for on-axis ECR heating to approximately 0.6 for the most external off-axis heating position.

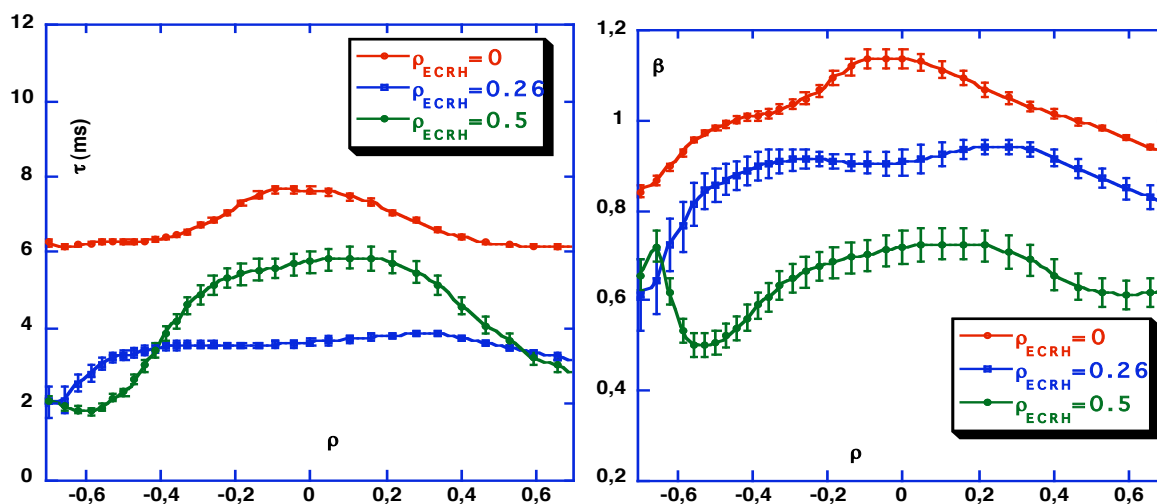


**Fig. 4.** Spatial dependence of  $\tau$  and  $\beta$  versus effective radius for three discharges with the ECR heating tuned at different rho's.

In conclusion, we observe significant changes in impurity confinement when we switch from ECR heating on-axis to off-axis. We will perform a detailed transport analysis to obtain more insight on the mechanisms responsible for these effects.

**Acknowledgements.** This work was partially funded by the Spanish Ministry of Science and Technology under Project No. FTN 2003-0905.

## References

- [1] R. Burhenn et al., Proc. 24<sup>th</sup> EPS Conf. **IV**, 1609 (1997).
- [2] R. Burhenn *et al.*, Rev. Sci. Instrum. **70**, 603 (1999).
- [3] R. Dux, R. Neu, A. G. Peeters et al., Plasma Phys. Control. Fusion **45**, 1815 (2004).
- [4] H. Nozato, S. Morita, M. Goto, et al., Phys. Plasmas **11**, 1920 (2004).
- [5] B. Zurro, M. A. Ochando, A. Baciero et al., Rev. Sci. Instrum. (to be published) (2004).
- [6] B. Zurro, M. A. Ochando, A. Baciero et al., Proc. 30<sup>th</sup> EPS Conf. **27A**, 2P.79.